Model Set Identification and Seismic Response Control of Flexible Structure

Hiroaki Fukushima[1] Wu Yue[1] Toshiharu Sugie[1]
Gi-Hwan Bae[2] Yoshiyuki Suzuki[2]

Abstract

In this paper, we perform the seismic control experiment of a flexible structure in order to investigate applicability of the model set identification methods to robust controller design. From the viewpoint of application to robust control, we identify model sets based on nominal models represented by rational transfer functions, in contrary to most existing methods based on affinely parameterized functions which tend to be high order functions. Also, we derive a less conservative error bound which takes account of low correlation properties of input signals. Based on the model set identification method and the $\mathcal{H}_\infty$ controller design method based on LMIs, we show that a closed-loop system which satisfies given design specifications is obtained systematically.

1 Introduction

In robust control system design, we need a model set of the true plant which consists of a nominal model and its norm-bounded uncertainty. Therefore, identification methods of model sets which are compatible with robust control framework have received much attention, see, *e.g.* [1]∼[7] . One of the most distinguished features of these methods compared with traditional probabilistic/statistical identification[8] is that they consider the estimation error is due to not only measurement noises but also unmodeled dynamics. Another important feature of these methods is that they evaluate error bounds of nominal models, which are essential in most of robust controller design methods, by using the given experimental data and *a priori* information on the plant. Therefore, it is expected that the model set identification methods make it possible to obtain a robust controller design more systematically. However, in contrast to much theoretical development which has been made in the past ten years, few experimental studies have been reported on model set identification and its application to the robust control system design. In most of robust controller design applications, the plant model set are constructed skillfully by the designers of great experience.

One of the practical difficulties of many model set identification methods is that the identified error bounds tend to be conservative. Although recent studies (see *e.g.* [9]∼[14]) try to reduce the conservativeness by integrating the probabilistic identification framework, the validity of these methods in the practical situation is still unclear. Another difficulty of most of these methods is that, because of computational complexity, the nominal model is limited to affinely parameterized functions which tend to be high order functions.

The main purpose of this paper is to investigate applicability of the model set identification methods to robust controller design by the experimental studies on seismic control of a flexible structure. From the viewpoint of application to robust control, we identify model sets based on nominal models represented by rational transfer functions. Also, we derive a less conservative error bound which takes account of low correlation properties of input signals. Based on the model set identification method and the $\mathcal{H}_\infty$ controller design method based on LMI, we show that a closed-loop system which satisfies given design specifications is obtained systematically.

In this paper, we use the following notations. For a vector $x \in \boldsymbol{C}^n$, we define $\|x\|_\infty := \max_{1\le i\le n} |x_i|$ and $\|x\| := \sqrt{\sum_{i=1}^n |x_i|^2}$, where x_i denotes the i-th element of x. The Hardy space of bounded analytic functions in $|z| > 1$ is denoted by $\mathcal{H}_\infty$, The real rational subspace of $\mathcal{H}_\infty$ is denoted by $\mathcal{RH}_\infty$. For a system $G(z) \in \mathcal{H}_\infty$, let $\|G\|_\infty$ denote $\mathcal{H}_\infty$ norm.

2 Model set identification method

In this section, we describe the model set identification method which is applied to the experimental study. This method first obtains the frequency-domain data and their residual bounds using the experimental I/O data and *a priori* information on the true plant, as described in Section 2.2. And then, the model sets based on the nominal mod-

[1]Department of Systems Science, Kyoto University, Uji, Kyoto 611-0011, Japan.
[2]Disaster Prevention Research Institute, Kyoto University, Uji, Kyoto 611-0011, Japan.

els represented by rational transfer functions are identified by using the frequency-domain data, as described in Section 2.3.

2.1 Model Description

Consider the following linear shift-invariant stable SIMO system affected by additive noise

$$y(t) = P_{id}(z)u(t) + v(t), \tag{1}$$

where z is the shift operator, $u(t)$ is an L-periodic scalar input signal and $y(t) \in \boldsymbol{R}^\ell$ is output vector corrupted by an additive noise $v(t) \in \boldsymbol{R}^\ell$. The transfer function of the true plant $P_{id}(z)$ is assumed to belong to the following system set given *a priori*

$$\mathcal{P} = \left\{ P(z) = \sum_{k=0}^{\infty} h(k) z^{-k} \,\middle|\, \|h(k)\|_\infty \le M\rho^k, \forall k \right\}. \tag{2}$$

Also, we assume that the experimental data $\{u(t), y(t)\}_{t=-N_s}^{N-1}$ is given, where $N = KL$ for an integer K.

For the true system $P_{id}(z)$, we consider the following model set

$$\boldsymbol{\Pi}(P_m, W) = \{P \mid P = P_m + \Delta W,\ \Delta \in \boldsymbol{\Delta}\}, \tag{3}$$

where $P_m(z) \in \mathcal{RH}_\infty$ is the n-th order nominal model described by

$$P_m(z) := B(z)A(z)^{-1}, \tag{4}$$

where

$$A(z) := 1 + a_1 z^{-1} + \cdots + a_n z^{-n} \tag{5}$$

$$B(z) := [B_1(z), B_2(z), \cdots, B_\ell(z)]^T, \tag{6}$$

$$B_i(z) := b_{i0} + b_{i1} z^{-1} + \cdots + b_{in} z^{-n}. \tag{7}$$

We define the coefficient vector

$$\theta := [a_1, \cdots, a_n, b_{10}, \cdots, b_{1n}, b_{\ell 1}, \cdots, b_{\ell n}]^T \tag{8}$$

Also, $W(z) \in \mathcal{RH}_\infty$ is a given scalar weighting function and $\Delta(z)$ is an unstructured uncertainty which belongs to the following set

$$\boldsymbol{\Delta} := \{\Delta(z) \in \mathcal{H}_\infty \mid \|\Delta(z)\|_\infty \le \gamma\}. \tag{9}$$

2.2 Frequency-domain data set

First, the following correlation sequences are obtained using the given experimental data $\{u(t), y(t)\}_{t=0}^{N-1}$

$$\{r_{uy}^N(\tau), r_{uu}^N(\tau)\}_{\tau=0}^{L-1}, \tag{10}$$

where

$$r_{uy}^N(\tau) := \frac{1}{N} \sum_{t=0}^{N-1} u(t-\tau)y(t), \tag{11}$$

$r_{uu}^N(\tau)$ and $r_{uv}^N(\tau)$ are defined in the same way as (11).

And then, we obtain the discrete Fourier transform(DFT) of $r_{uy}^N(\tau)$ and $r_{uu}^N(\tau)$ in (10)

$$\{S_{uy}^L(\omega_k), S_{uu}^L(\omega_k)\}_{k=0}^{L-1}, \tag{12}$$

where $\omega_k = 2\pi k/L$, and we define DFT of $\{r_{uv}^N(\tau)\}_{\tau=0}^{L-1}$ as $\{S_{uv}^L(\omega_k)\}_{k=0}^{L-1}$.

Now, since $u(t)$ is L-periodic, the following input-output equation is satisfied.

$$S_{uy}^L(\omega_k) = P_{id}(\omega_k)S_{uu}^L(\omega_k) + R(\omega_k) \qquad k = 0, \cdots, L-1, \tag{13}$$

where $R(\omega_k)$ is the residual

$$R(\omega_k) := S_{uv}^L(\omega_k) + E(\omega_k), \tag{14}$$

$S_{uv}^L(\omega_k)$ is the term due to the noise, and also we have an additional residual term $E(\omega_k)$ because the system is not in steady state at $t = 0$. $P_{id}(\omega_k)$ is the frequency response of $P_{id}(z)$ for $z = e^{j\omega_k}$.

An upper bound of $\|E(\omega_k)\|$ is given in the following proposition.

Proposition 1 *An upper bound of* $\|E(\omega_k)\|$ *is given as* ξ,

$$\xi = \frac{\sqrt{\ell} M \rho^{N_s}(1-\rho^N)}{N(1-\rho^L)}(c_1 + c_2), \tag{15}$$

where

$$c_1 := \sum_{\tau=0}^{L-1} \sum_{j=1}^{L-1} \rho^j |\phi_u(\tau, j)| \tag{16}$$

$$c_2 := \sum_{\tau=0}^{L-1} \sum_{n=1}^{L} \frac{\rho^{L+n-1}}{(1-\rho^L)} \left| r_{uu}^L(-N_s - 1 + \tau - n) \right| \tag{17}$$

$$\phi_u(\tau, j) := \sum_{i=0}^{j} u(-\tau + i)u(-N_s - j + i) \tag{18}$$

The upper bound in (15) decays exponentially as N_s grows. Also, it is important to note that the conservativeness is reduced in the case where the input signals $u(t)$ are low-correlated because of $|r_{uu}^L(-N_s - 1 + \tau - n)|$ in (17) and $\phi_u(\tau, j)$ in (16). This is a distinguished feature compared with the existing bound [11], which does not take account of the correlation properties of the input signals.

On the other hand, we consider the following upper bound of $\|S_{uv}^L(\omega_k)\|$, which takes account of a low correlation property of $v(t)$[14],

$$\|S_{uv}^L(\omega_k)\| \le \zeta_k := \sqrt{\frac{\eta \ell L S_{uu}^L(\omega_k)}{N}}. \tag{19}$$

Note that some discussions on the choice of η in the case when $v(t)$ is a Gaussian white noise are given in [14].

From (14), (15) and (19), an upper bound of the residual $\|R(\omega_k)\|$ is given as

$$\lambda_k := \xi + \zeta_k. \tag{20}$$

Using λ_k, we define the residual set

$$\mathcal{R}_k := \{R(\omega_k) \mid \|R(\omega_k)\| \leq \lambda_k\}, \tag{21}$$

for each k.

In our model set identification method, we use the frequency-domain data in (12) and its residual bound λ_k in (20). In (20), ξ decays exponentially as N_s grows, while ζ_k decays as N grows. However, the total length of the experiment is limited in practical situations. Therefore, N_s and N should be chosen appropriately, such that λ_k is as small as possible for the given total data length.

2.3 Identification method

From (3), eq.(13) can be written as

$$S^L_{uy}(\omega_k) = P_m(\omega_k)S^L_{uu}(\omega_k) + \Delta(\omega_k)W(\omega_k)S^L_{uu}(\omega_k) + R(\omega_k) \tag{22}$$

Therefore, an upper bound of $\|\Delta(\omega_k)\|$ is described using the given frequency-domain data as

$$\delta_k := \frac{\|S^L_{uy}(\omega_k) - P_m(\omega_k)S^L_{uu}(\omega_k)\| + \lambda_k}{|W(\omega_k)|S^L_{uu}(\omega_k)}, \quad \forall\omega_k \tag{23}$$

We consider the identification problem of the following P_m, which minimizes the peak of δ_k

$$P_m = \arg\min_{\theta\in R^n} \max_k \gamma, \tag{24}$$

$$s.t. \quad \delta_k \leq \gamma, \quad \forall k \tag{25}$$

We note that, the model set obtained by the optimization problem in (24) and (25) is the smallest one such that there exists a $\Delta(z) \in \boldsymbol{\Delta}$ which satisfies (22) for any $R(\omega_k) \in \mathcal{R}_k$. Therefore, this model set is unfalsified by the given frequency-domain data in (12) in terms of the model validation methodology [15][16]. Also, note that, since this identification algorithm takes account of the worst-case error bounds at the only given discrete frequency points ω_k, the obtained model set is practical for robust control by choosing L as an appropriately large value.

The problem in (24) is equivalent to identify the following θ and γ

$$\theta = \arg\min_{\theta\in R^n} \gamma$$
$$s.t. \ \|A(\omega_k)S^L_{yu}(\omega_k) - B(\omega_k)(\omega_k)S^L_{uu}(\omega_k)\| \leq |A(\omega_k)W(\omega_k)|\left(\gamma S^L_{uu}(\omega_k) - \lambda_k\right), \forall\omega_k \tag{26}$$

Since this is a nonlinear optimization problem, it is difficult to obtain the global optimal solution. Therefore, we consider the following iterative algorithm.

Step 1 Fix $A(\omega_k) = 1$ and $\lambda_k = 0$ on the right hand side in (26). Then obtain $A_1(z)$ and $B_1(z)$ by computing θ in (26) via convex optimization.

Step 2 Fix $A(\omega_k) = A_1(\omega_k)$ on the right hand side in (26). Then obtain $A_2(z)$, $B_2(z)$ and γ by computing θ in (26) via convex optimization.

Step i Similarly to Step2, identify $A_i(z)$, $B_i(z)$ and γ for $A(\omega_k) = A_{i-1}(\omega_k)$ on the right hand side in (26).

In the case where we have $A_{i-1}(\omega_k) \simeq A_i(\omega_k)$ by the iteration, the nominal model $P_m(z)$ and γ identified using this iterative algorithm are expected to be a good approximate of the exact optimal solution of the problem in (26).

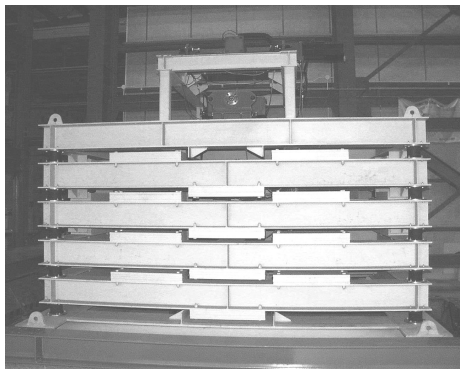

Figure 1: Flexible structure

3 Model set ID and control of flexible structure

3.1 Outline of experimental system

The five-story frame structure at the Disaster Prevention Research Institute, Kyoto University[17] is depicted in Fig.1. This system is $2.3m$ high and $12t$ in weight. The dimensions of the shaking table are $5.0m \times 3.0m$. The Active Mass Damper(AMD) systems are installed on the roof in order to suppress the seismic disturbances from the shaking table. The AMD has a mass which is driven linearly through an ball screw by an AC servo motor. Note that we use only one AMD in the experiments, although two AMD systems crossing each other are installed on the roof. The acceleration of the 5th floor and the 4th floor, and the stroke of the AMD are measured in this study. Therefore, the experimental system can be described as the following continuous time system:

$$y_c(t) = P_c(s)u_c(t) + d(t), \tag{27}$$
$$u_c(t) = C(s)y_c(t), \tag{28}$$

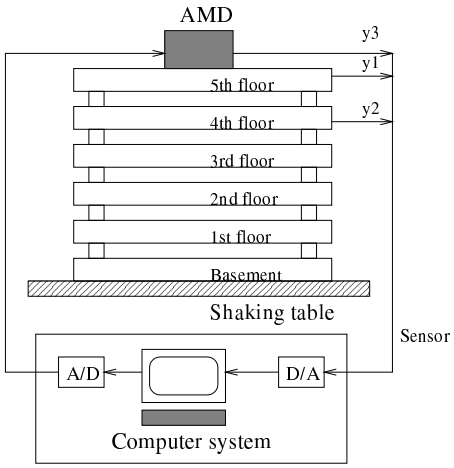

Figure 2: Experimental system

where $d(t)$ is the seismic disturbance from the shaking table and $C(s)$ is the controller which is obtained in Section 3.3. The output vector of the closed loop system $y_c(t) := [y_1^T(t)\ y_2^T(t)\ y_3^T(t)]^T$ is composed of the acceleration of the 5th floor and the 4th floor relative to the ground, defined by $y_1(t)$ and $y_2(t)$ respectively, and the stroke of the AMD $y_3(t)$. The control input $u_c(t) \in \boldsymbol{R}$ is generated by the inertia force of the moving mass on the 5th floor.

Since $y_3(t)$ is the displacement of the AMD relative to the 5th floor, the transfer function vector P_c in (27) can be described as

$$P_c(s) = \begin{bmatrix} P_1(s) \\ P_2(s) \\ \frac{1}{s^2}(P_3(s) - P_1(s)) \end{bmatrix}, \qquad (29)$$

where $P_1(s)$ and $P_2(s)$ are the transfer function from $u_c(t)$ to $y_1(t)$ and $y_2(t)$ respectively, and $P_3(s)$ is the transfer functions from $u_c(t)$ to the acceleration of the moving mass relative to the ground. In this study, we have *a priori* information that $P_3(s)$ is well approximated by the given constant

$$P_{m3} := \frac{m_a}{m_a l_a/2\pi + 2\pi J_a/l_a}, \qquad (30)$$

where J_a is the moment of inertia of the motor and l_a is the lead length of the ball screw. Therefore, we identify a nominal model $P_m(s)$ and its error bound $W(s)$ of the following $P_{id}(s)$

$$P_{id}(s) := [P_1(s), P_2(s)]^T, \qquad (31)$$

as described in Section 3.2. And in Section 3.3, based on $P_m(s)$, P_{m3} and $W(s)$, we design a controller which guarantees robust stability and also makes the sensitivity to the seismic disturbance small in the low frequency range.

3.2 Model set identification

In our model set identification problem, the true plant is described as (1), where $P_{id}(z)$ denotes the z-transform of $P_{id}(s)$ in (31) with sampling time $0.01s$. We perform impulse response experiments and choose M and ρ in (2) as $M = 650$ and $\rho = 0.985$. Fig.3 shows the impulse response of y_1 which is the average of the results of seven experiments by the solid line and also shows its bound $M\rho^\tau$ by the broken line. From Fig.3, we can observe that M and ρ are chosen such that $M\rho^\tau$ is a reasonably conservative bound, and $P_{id}(z)$ has very small decay rate $\rho^{-1} \simeq 1.015$. On the other hand, the constant η in (19) is chosen as $\eta = 0.264$ according to the noise data $v(t)$ observed with the input $u(t) = 0$.

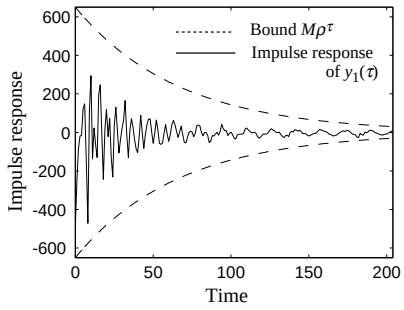

Figure 3: Impulse response and its bound

The input signal is chosen as a filtered pseudo-random binary sequence(PRBS)

$$u(t) = F(z)\widetilde{u}(t), \qquad (32)$$

where $\widetilde{u}(t)$ is a PRBS with period 2047 and $F(z)$ is the z-transform of the band-path filter

$$F(s) = \frac{1}{(s/3+1)^2(s/25+1)^2} \qquad (33)$$

The input-output data are observed with sampling interval $0.01s$, and then we obtain $\{u(t), y(t)\}$ for identification with sampling interval $0.1s$ and the period $L = 205$ by decimation. Therefore, the length of the total obtained data$(N_s + N)$ is $5L = 1025$.

The design parameters N and N_s are chosen as $N_s = 4L$ and $N = L = 205$ according to the value of λ_k in (20), as described in Section 2.2. Table 1 shows the relationship between λ_k and N_s. Table 1 indicates that N_s should be chosen as a large value, since this experimental system has small decay rate ρ^{-1}. And also, we show the values of the existing bounds[11]. From this result, the bounds given in (15) are less conservative than the existing bound.

In the situation stated above, we now apply the identification algorithm with ten iterations. Since

Table 1: Residual bound level ($\max_k \lambda_k$)

N_s	205	410	615	820
Proposed	9.8E−1	5.9E−2	4.0E−3	2.5E−4
Existing	7.6	4.3E−1	3.0E−2	2.9E−3

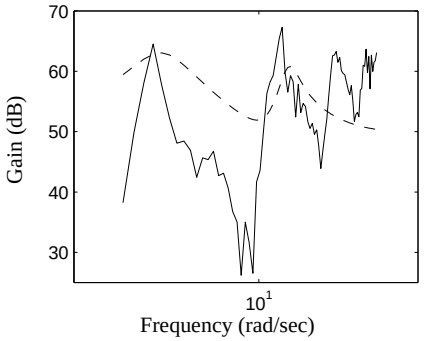

Figure 4: Gain plot of P_m (1st iteration)

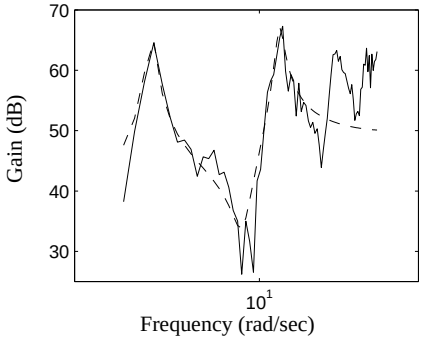

Figure 5: Gain plot of P_m (10th iteration)

our goal is control system design which makes the sensitivity to the seismic disturbance small in the low frequency range and also guarantee the robust stability mainly for the model uncertainty in the high frequency range, the weighting function $W(z)$ in(3) is chosen as the z-transform of the low-cut filter

$$W(s) = \frac{(s/20+1)^6}{(s/250+1)^6} \tag{34}$$

in order that the model error is small in the frequency range.

The gain plots of the model error of the identified fourth order nominal models on the first iteration and the tenth iteration are shown in Fig.4 and Fig.5 respectively. The broken line shows the gain plots of the identified transfer function from $u(t)$ to $y_1(t)$ and the solid line shows the spectrum estimates $|S_{uy_1^L}(\omega_k)|/S_{uu}^L(\omega_k)$. From these figures, we can see the performance of the nominal model is improved by the proposed iteration algorithm particularly in the low frequency range.

Also, the uncertainty bound $\gamma|W(\omega_k)|$ on the the tenth iteration are shown in Fig.6. The broken line shows the uncertainty bound $\gamma|W(\omega_k)|$ and the solid line shows the nonparametric error bound $\delta_k|W(\omega_k)|$ in (23). In Fig.6, $\gamma|W(\omega_k)|$ is a tight bound of $\delta_k|W(\omega_k)|$ particularly in the low frequency range.

From Fig.5 and Fig.6, we can see that a good model set which reflects our requirements described in (24) and (25) is obtained.

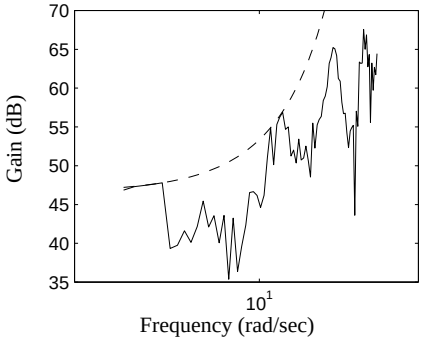

Figure 6: Error bounds (10th iteration)

Note that, since the weighting function in (34) is of high order, we use the second order function $W_1(z)$, which bounds $\delta_k|W(\omega_k)|$ as tight as possible, in the controller design step in Section 3.3. Note that the bilinear transforms $P_m(s)$ and $W_1(s)$ of $P_m(z)$ and $W_1(z)$ are used in Section 3.3.

3.3 Controller Design

In this section, we design a controller based on the following specifications:

i) Suppress the acceleration for the first and the second modes.

ii) Guarantee the robust stability for the model set identified in Section 3.2.

iii) Keep the stroke of the moving mass of the AMD system within range $\pm 30cm$.

We formulate the specification i), ii) and iii) in the framework of the $\mathcal{H}_\infty$ control based on the system shown in Fig.7. In this figure, $W_1(s)$ is the z-transform of the weighting function obtained in Section.3.2. Since the disturbance $d(t)$ from the shaking table has the same mode as the response from the AMD, $W_2(s)$ is chosen as

$$W_2(s) = \frac{1}{\epsilon}\left(\sum_{i=1}^{2} \frac{p_i\overline{p}_i}{(s+p_i)(s+\overline{p}_i)},\right)\begin{bmatrix} 1 \\ 1 \\ 1/s^2 \end{bmatrix} \tag{35}$$

where p_i and $\overline{p}_i$ are the pole of the nominal model $P_m(s)$. Also, W_3 is chosen as a diagonal matrix

$$W_3 = \mathrm{diag}(20, 20, 1). \tag{36}$$

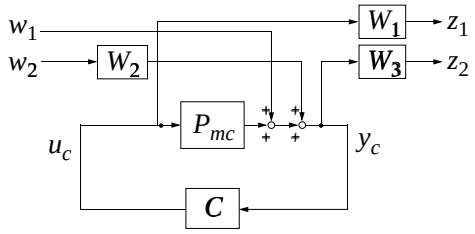

Figure 7: Feed-back system

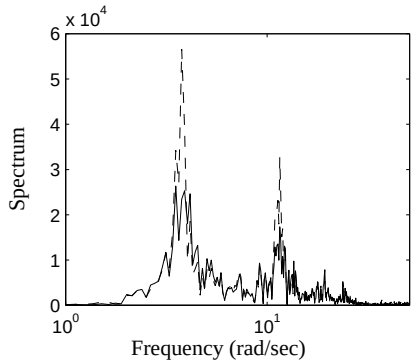

Figure 8: Control performance in frequency domain

Based on the formulation in Fig.7, our design specification is described as the following design problem of $C(s)$.

$$C(s) = \arg\min_{C} \epsilon,$$
$$s.t. \quad \|T_{z1w1}\|_\infty \leq 1, \quad \|T_{z2w2}\|_\infty \leq 1, \quad (37)$$

where $T_{z1w1}(s)$ denotes the transfer function from w_1 to z_1 and $T_{z2w2}(s)$ denotes the transfer function from w_2 to z_2. Since it is difficult to get the exact optimal solution, we obtain $C(s)$ based on a design method[18] which gives an upper bound of the optimal ϵ based on the linear matrix inequalities(LMIs).

For the obtained closed-loop system, we perform the seismic control experiment. The El Centro earthquake wave of the North-South direction scaled down to the maximum acceleration 100gal is used as the disturbance from the shaking table. Fig.8 shows the control effect in frequency-domain by the DFT of the acceleration of the 5th floor. The solid line shows the spectrum of the seismic response of the designed closed-loop system. On the other hand, the broken line shows the one without control. From Fig.8, we can see that our controller reduces the peak of the spectrum for the first and the second mode.

The experimental results shown in this section indicate that, a closed-loop system which satisfies our design specification is systematically obtained based on the model set identification method and the $\mathcal{H}_\infty$ controller design method based on LMI. Although the obtained controller is still conservative because of computational complexity of the robust controller design method, it is practical as the first step for practical model set identification.

References

[1] Special Issue on System Identification for Robust Control Design, *IEEE Trans. Automat. Contr.*, **AC-37**-7, pp. 899-1008 (1992)

[2] B. Ninness and G.C. Goodwin: Estimation of Model Quality, *Automatica*, **31**-12, 1771/1797 (1995)

[3] R.S.Smith and M.Dahleh(Eds): The Modeling of Uncertainty in Control Systems, Proc. 1992 Santa Barbara Workshop, Springer-Verlag, Berlin.

[4] L. Giarrè and M. Milanese: SM identification of approximating models for H_∞ robust control; *IEEE Conf. Decision. Contr.*, pp. 4184-4189 (1996)

[5] L. Giarrè, M. Milanese and M.Taragna: H_∞ Identification and Model Quality Evaluation; *IEEE Trans. Automat. Contr.*, **AC-42**, pp. 188-199 (1997)

[6] T. Zhou and H. Kimura: Simultaneous Identification of Nominal Model, Parametric Uncertainty and Unstructured Uncertainty for Robust Control; *Automatica*, **30**-3, pp. 391-402 (1994)

[7] Robert L. Kosut: Iterative Adaptive Robust Control via Uncertainty Model Unfalsification; *Proc of IFAC 13rd World Congress*, pp. 91-96 (1996)

[8] L. Ljung: System Identification, Theory for the User Englewood Cliffs, NJ, Prentice-Hall (1987)

[9] F. Paganini: A Set-Based Approach for White Noise Modeling; *IEEE Trans. Automat. Contr.*, **AC-41**, pp. 1452-1465 (1996)

[10] S. R. Venkatesh, M. A. Dahleh: Identification in the Presence of Classes of Unmodeled Dynamics and Noise; *IEEE Trans. Automat. Contr.*, **AC-42**, pp. 1620-1635 (1997)

[11] D. K. De Vries and P. M. J. Van den Hof: Quantification of uncertainty in transfer function estimation: a mixed probabilistic-worst-case approach; *Automatica*, Vol.30, No.3, pp. 543-557 (1995)

[12] G. C. Goodwin, M Gevers and B. Ninness: Quantifying the error in estimated transfer functions with application to model order selection; *IEEE Trans. Automat. Contr.*, **AC-37**, pp. 913-928 (1992)

[13] M. Milanese and M. Taragna: H_∞ identification of "soft" uncertainty models; *IEEE Conf. Decision. Contr.*, pp. 2418-2423 (1996)

[14] H. Fukushima and T. Sugie: Model Set Identification Based on Periodgrams; *Proc of IFAC 14rd World Congress*, pp. 547-552 (1999)

[15] R. Smith, S. Rangan, K. Poolla: Control-Oriented Model Validation; *Proc. of IFAC Symposium on System Identification*, 443/450 (1997)

[16] J. Chen: Frequency-Domain Tests for Validation of Linear Fractional Uncertain Models; *IEEE Trans. Automat. Contr.*, **AC-42**, pp. 748-760 (1997)

[17] M. Yamamoto and Y. Suzuki: Experimental Study of an Active Mass Damper with Variable Gain Control Algorithm; *Proc. 2nd World Conference on Structural Control*, pp. 775-784 (1998)

[18] I. Masubuchi, A. Ohara and N. Suda LMI-based Controller Synthesis: A Unified Formulation and Solution; *Int. j. Robust and Nonlinear Contr.*, pp. 669-686 (1998)